

# MRI features of breast lymphoma: preliminary experience in seven cases

Lijun Wang  
Dengbin Wang  
Weimin Chai  
Xiaochun Fei  
Ran Luo  
Xiaoxiao Li

## PURPOSE

We aimed to evaluate the imaging features of breast lymphoma using magnetic resonance imaging (MRI).

## METHODS

This retrospective study consisted of seven patients with pathologically confirmed breast lymphoma. The breast lymphomas were primary in six patients and secondary in one patient. All patients underwent preoperative dynamic contrast-enhanced MRI and one underwent additional diffusion-weighted imaging (DWI) with a b value of 600 s/mm<sup>2</sup>. Morphologic characteristics, enhancement features, and apparent diffusion coefficient (ADC) values were reviewed.

## RESULTS

On MRI, three patients presented with a single mass, one with two masses, two with multiple masses, and one with a single mass and a contralateral focal enhancement. The MRI features of the eight biopsied masses in seven patients were analyzed. On MRI, the margins were irregular in six masses (75%) and spiculated in two (25%). Seven masses (87.5%) displayed homogeneous internal enhancement, while one (12.5%) showed rim enhancement. Seven masses (87.5%) showed a washout pattern and one (12.5%) showed a plateau pattern. The penetrating vessel sign was found in two masses (25%). One patient with two masses underwent DWI. Both masses showed hyperintense signal on DWI with ADC values of  $0.867 \times 10^{-3}$  mm<sup>2</sup>/s and  $0.732 \times 10^{-3}$  mm<sup>2</sup>/s, respectively.

## CONCLUSION

Breast lymphoma commonly presents as a homogeneously enhancing mass with irregular margins and displays a washout curve pattern on dynamic MRI. A low ADC value may also indicate a possible diagnosis of breast lymphoma.

**B**reast lymphoma, which constitutes only 0.04%–0.5% of all breast malignancies (1), can be divided into primary or secondary breast lymphoma (2). The majority of breast lymphomas are diffuse large B-cell lymphoma (3). The spontaneous regression of a breast lymphoma is rare and the five-year overall survival rate is 53% (1, 4). Early-stage identification and the use of radiotherapy are favorable prognostic factors, while mastectomy is associated with a poorer survival (1, 5). Therefore, a preoperative diagnosis of breast lymphoma would mean an earlier diagnosis and likely avoid unnecessary aggressive procedures.

Previous studies demonstrated mammographic and ultrasonographic findings of breast lymphoma (6–8). Most lesions were high-density masses without spiculated margins and calcifications on mammography and noncircumscribed hypoechoic masses on ultrasonography (6–8). However, none were pathognomonic.

Data on the magnetic resonance imaging (MRI) of breast lymphoma are limited to some single case reports (4, 7, 9–19) and small sample size case series (8, 20–23). The morphology and time-signal intensity curve (TIC) of breast lymphoma on MRI are variable. Diffusion-weighted imaging (DWI) is a functional imaging technique that is useful for distinguishing lymphoma from other malignant tumors in other systems (24, 25). However, to the best of our knowledge, the value of DWI in differentiating breast lymphoma from other malignant breast lesions has not been discussed. Therefore, the purpose of this study is to assess the MRI and DWI features of breast lymphoma.

From the Department of Radiology (L.W., D.W. ✉ [dbwang8@aliyun.com](mailto:dbwang8@aliyun.com), R.L., X.L.) Xinhua Hospital, Shanghai Jiao Tong University School of Medicine, Shanghai, China; the Departments of Radiology (W.C.) and Pathology (X.F.), Ruijin Hospital, Shanghai Jiao Tong University School of Medicine, Shanghai, China.

Received 26 December 2014; revision requested 26 January 2015; final revision received 21 April 2015; accepted 23 May 2015.

Published online 17 September 2015.  
DOI 10.5152/dir.2015.14534

## Methods

### Patient selection

This retrospective study evaluated all women with pathologically confirmed breast lymphoma in our hospital between July 2009 and July 2014. Seven women were included in the analysis (median age, 56 years; range, 47–79 years). In all patients, the diagnosis of breast lymphoma was confirmed by core needle biopsy (n=4) or lumpectomy (n=3). The histologic type was diffuse large B-cell lymphoma in all patients. All patients underwent a preoperative MRI and provided written informed consent prior to the biopsy or lumpectomy. According to the criteria proposed by Wiseman et al. (2), one case (case 5) was classified as secondary breast lymphoma, and the remainder as primary breast lymphoma. The institutional review board of our hospital approved this clinical research. Written informed consent was waived for this retrospective study.

### Imaging protocol

A 1.5 T dedicated spiral breast MRI system (Aurora Systems) with a single channel quadrature breast coil or a 3.0 T whole body MRI scanner with an eight-channel phase-array breast coil (Signa HDxt; GE Healthcare) were used. For dynamic imaging, gadolinium-diethylenetriamine pentaacetic acid (Gd-DTPA, Magnevist, Bayer-Schering Pharma AG) of 0.2 mmol/kg body weight was administered intravenously at a rate of 2 mL/s followed by 20 mL normal saline flush (26). MRI of six patients (case 1–6) was performed using a 1.5 T MRI system with dynamic imaging only. The spiral axial screen mode was

used. Dynamic imaging of both breasts was obtained before and at 180 s, 360 s, and 540 s after the injection of Gd-DTPA. The parameters for this sequence were as follows: TR/TE, 4.8/29 ms; slice thickness, 1.125 mm; gap, 0 mm; matrix, 360×360×128. One patient (case 7) was imaged using a 3 T whole-body MRI scanner. The following sequences were performed: axial short tau inversion recovery (STIR) (TR/TE, 7060/35.2 ms; TI, 170 ms; slice thickness, 4 mm; gap, 1 mm; matrix, 320×192); axial DWI, b=600 s/mm<sup>2</sup> (TR/TE, 5950/64.6 ms; slice thickness, 4 mm; gap, 1 mm; matrix, 160×160); Volume Image Breast Assessment (VIBRANT) sequence (GE Healthcare) with images obtained before and at 54 s, 108 s, 162 s, 216 s, and 270 s after injection of Gd-DTPA (TR/TE, 4.3/2.1 ms; TI, 14 ms; slice thickness, 1.2 mm; gap, 0 mm; matrix, 416×320).

Each mammography examination was performed using a GE Senographe 2000D instrument (GE Healthcare) with routine craniocaudal and mediolateral oblique projections. Each ultrasonography examination was performed using a GE Logiq9 instrument (GE Healthcare).

### MRI analysis

Eight masses were biopsied in seven patients (both masses were biopsied in case 7). The imaging features of the biopsied masses were recorded for analysis. Two breast radiologists (D.W., 20 years experience; L.W., four years experience) retrospectively reviewed all images in consensus. The mass size was determined by measuring the maximum diameter on MRI. The morphology and TIC of the lesion was classified according to the Breast Imaging Reporting and Data System (BI-RADS) MRI lexicon (27). For the TIC, the initial phase of enhancement was rated as slow (<50% increase in signal intensity), medium (50%–100% increase in signal intensity), and fast (>100% increase in signal intensity) in the first two minutes or when the curve starts to change. Delayed phase was the enhancement pattern after two minutes or after the curve starts to change (27). Delayed phase enhancement was rated as persistent (continued >10% increase in signal over time), plateau (signal intensity does not change over time after its initial rise) and washout (signal intensity decreases >10% after its highest point from its initial rise) (27).

Post-processing included subtraction of the precontrast images from the dynamic axial T1 sequence on a pixel-by-pixel basis; the TIC was obtained on both scanners. Regions of interest (ROIs) for the TIC were set on the lesion and avoided cystic regions. For the Aurora imaging system, although the time of acquisition of each sequence was 180 s, the center of the 3D k-space cube was filled at 90 s after initiation of acquisition. So the three time points for the three postcontrast sequences on the TIC were 90 s, 270 s, and 450 s. The DWI and apparent diffusion coefficient (ADC) value mapping were analyzed on a workstation (GE Healthcare) for the 3.0 T MRI system. Three 55–80 mm<sup>2</sup> ROIs were set on the lesion without cystic regions. The average value of three measurements was used as the ADC value. The adjacent vessel sign was assessed as positive if a vessel either entering a lesion or in contact with a lesion's edge could be clearly delineated on any of the subtracted images (28, 29). Penetrating vessel sign was assessed as positive if a vessel was identified as passing through a lesion on early dynamic MRI images (21).

### Statistical analysis

Analyses were performed using the SPSS 19.0 (IBM Corp) analysis software package. The age, lesion size, and duration were shown as median (minimum–maximum) because of limited sample size.

## Results

The clinical characteristics and traditional imaging findings of breast lymphoma are summarized in Table 1. Nipple enlargement was found in one patient (case 6) (Fig. 1). The duration between the initial report of clinical symptoms and the MRI examination was seven days (range, 2–180 days). The pathologic findings revealed that all of the tumors had an infiltrative growth pattern. There were no marked desmoplasia or scirrhous reactions in any of the lesions. The bone marrow biopsy was normal in all patients.

The MRI features of the histopathologically diagnosed breast lymphoma are summarized in Table 2. On MRI, three patients presented with a single mass, one patient with two masses, two patients with multiple masses, and one patient with a single

### Main points

- Breast lymphoma commonly presents as a homogeneously enhancing mass with irregular margins and displays a washout curve pattern on dynamic MRI.
- The infiltrative growth pattern instead of desmoplasia or scirrhous reactions might be responsible for the irregular or spiculated margins of breast lymphoma.
- A low apparent diffusion coefficient value could indicate a possible diagnosis of breast lymphoma.
- MRI may be more sensitive in detecting multifocal or multicentric lesions of breast lymphoma.

**Table 1. Clinical characteristics and traditional imaging findings of breast lymphoma**

Case number	Age (y)	Side	Clinical history	Duration <sup>a</sup> (days)	Mammography	Ultrasonography
1	56	Left	Palpable mass in left axilla with pain	30	Focal asymmetry	A hypoechoic mass, angular margin
2	79	Right	Palpable mass in breast with erythema	7	A high density mass, indistinct margin	A hypoechoic mass, angular margin
3	47	Left	Palpable mass in breast	2	A high density mass, obscured margin	A hypoechoic mass, angular margin
4 <sup>b</sup>	51	Bilateral	Palpable mass in breast	7	An equal density mass, obscured margin	A heterogeneous mass, well-defined margin
5	49	Right	Palpable mass in cervical region and subsequently in the breast	180	NA	A hypoechoic mass, angular margin
6	57	Right	Palpable mass in breast with erythema and nipple enlargement	30	Global asymmetry	NA
7	70	Right	Palpable mass in breast	2	Focal asymmetry	A hypoechoic mass, indistinct margin

NA, not available.  
<sup>a</sup>Duration was defined as the time between the initial report of clinical symptoms and the MRI examination.  
<sup>b</sup>This patient had undergone lumpectomy of the contralateral breast for mucosa-associated lymphoid tissue lymphoma three months previously.

**Table 2. MRI features of histopathologically diagnosed breast lymphoma in the current study**

Case number	Lesion	Size (cm)	Shape	Margin	Internal enhancement	Penetrating vessel sign	Initial phase	Delayed phase
1 <sup>a</sup>	Multiple masses	2.3	Oval	Irregular	Homogeneous	Absent	Medium	Washout
2	Single mass	4.7	Oval	Irregular	Rim enhancement	Absent	Medium	Washout
3	Single mass	2.7	Oval	Irregular	Homogeneous	Absent	Medium	Washout
4	Single mass	2.1	Oval	Irregular	Homogeneous	Present	Medium	Washout
5	Single mass, contralateral focal enhancement	4.7	Irregular	Spiculated	Homogeneous	Absent	Medium	Washout
6 <sup>a</sup>	Multiple masses	8.9	Irregular	Spiculated	Homogeneous	Present	Medium	Washout
7 <sup>b</sup>	Two masses	2.6	Oval	Irregular	Homogeneous	Absent	Fast	Washout
7	Two masses	1.6	Round	Irregular	Homogeneous	Absent	Fast	Plateau

<sup>a</sup>Imaging feature of the biopsied mass only.  
<sup>b</sup>Imaging features of the two biopsied masses in the right breast are presented separately.

mass and a contralateral focal enhancement. The median size of the lesions was 2.65 cm (range, 1.6–8.9 cm). On MRI, the mass shapes were oval in six (75%) and irregular in two (25%). The margins were irregular in six masses (75%) and spiculated in two (25%). Homogeneous internal enhancement was seen in seven masses (87.5%) and rim enhancement was seen in one (12.5%). Seven masses (87.5%) showed a washout pattern and one (12.5%) showed a plateau pattern. Most of the masses showed medium initial enhancement (n=6, 75%) and a washout curve pattern on the delayed phase (n=7, 87.5%). Adjacent vessel sign was positive in all cases; however, penetrating vessel sign was found in two cases only (25%). In case 7 (Fig. 2), two masses were detected on MRI and both of them showed hyperintense sig-

nal on DWI with ADC values of  $0.867 \times 10^{-3} \text{ mm}^2/\text{s}$  and  $0.732 \times 10^{-3} \text{ mm}^2/\text{s}$ , respectively.

## Discussion

Breast lymphoma most often occurs in females in the fifth or sixth decade of life (1–23) and is extremely rare in males (16). There was a right-sided predominance in our study. The median patient age in our study was 56 years and histologic type was diffuse large B-cell lymphoma in all patients consistent with findings in previous reports (1–8, 20–23). However, breast cancer also occurs in elderly women. The differential diagnosis between breast lymphoma and other malignant tumors remains a challenge. We performed this study to evaluate the clinical and MRI features of breast

lymphomas and identify useful diagnostic clues.

A palpable mass -the most common presenting sign in breast lymphoma- is sometimes accompanied by local pain and inflammatory changes (1–23). In our study, a palpable mass in the breast was found in six of seven patients, which was in accordance with the previous studies (1–23). Nipple enlargement was found in one patient and the lesion in the nipple resolved after chemotherapy. We postulate that the lesion in the nipple was due to tumor-cell infiltration, which differed from the nipple retraction in invasive ductal carcinomas because of desmoplastic and fibrotic reaction. To the best of our knowledge, except for the one patient with breast lymphoma localized in the nipple (19), this sign has not been described

**Table 3.** Review of magnetic resonance imaging characteristics of breast lymphoma in the literature

Reference	No. of patients and lesions	Morphology <sup>a</sup>	Margin of mass <sup>a</sup>	Internal enhancement <sup>a</sup>	TIC <sup>a</sup>
Oya et al. (4)	1, 2	Lobulated	Irregular	Heterogeneous	NA
Yang et al. (7)	1, 1	Lobulated	Irregular	Heterogeneous	Washout
Surov et al. (8)	8, 21	Mass (17), NME (4)	Well-defined (12), Irregular (5)	Homogeneous (14), heterogeneous (3)	Persistent (1), plateau (18), washout (1)
Mussurakis et al. (9)	1, 3	Irregular	Irregular	Heterogeneous, rim enhancement	Plateau
Darnell et al. (10)	1, 1	Lobulated	Well-defined	Heterogeneous	NA
Demirkazik (11)	1, multiple	Round, oval	Well-defined	Rim enhancement	Washout
Espinosa et al. (12)	1, multiple	Multiple foci	Irregular	Homogeneous	Persistent
Woo et al. (13)	1, 2	Round	Well-defined	Heterogeneous	Washout
Zechmann et al. (14)	1, multiple	1 mass, 1 NME	Well-defined	Heterogeneous	Plateau
Adrada et al. (15)	1, multiple	Lobulated, irregular	Irregular	Heterogeneous, rim enhancement	NA
Rathod et al. (16)	1, 1	Lobulated	Well-defined	Homogenous	Plateau
Jinming et al. (17)	1, 2	Oval	Well-defined	Homogeneous	Plateau, washout
Uematsu et al. (18)	1, multiple	Irregular	Well-defined, irregular	Rim enhancement	Persistent
Nakatsuka et al. (19)	1, 1	Lobulated	Well-defined	Heterogeneous	NA
Rizzo et al. (20)	7, 7	Mass (6), NME (1)	Irregular (3), well-defined (2), spiculated (1)	Homogeneous (2), heterogeneous (2), rim enhancement (2)	Plateau (5), washout (2)
Matsubayashi et al. (21)	3, 3	Lobulated (3)	Well-defined (3)	Homogeneous (3)	NA
Liu et al. (22)	20, 82	Mass (11), NME (7), mixed type (2)	Irregular (26), well-defined (12)	Heterogeneous	Persistent (5), plateau (21), washout (12)

TIC, time-signal intensity curve; NA, not available; NME, nonmass enhancement.  
<sup>a</sup>The number in parentheses represents the number of reported cases.

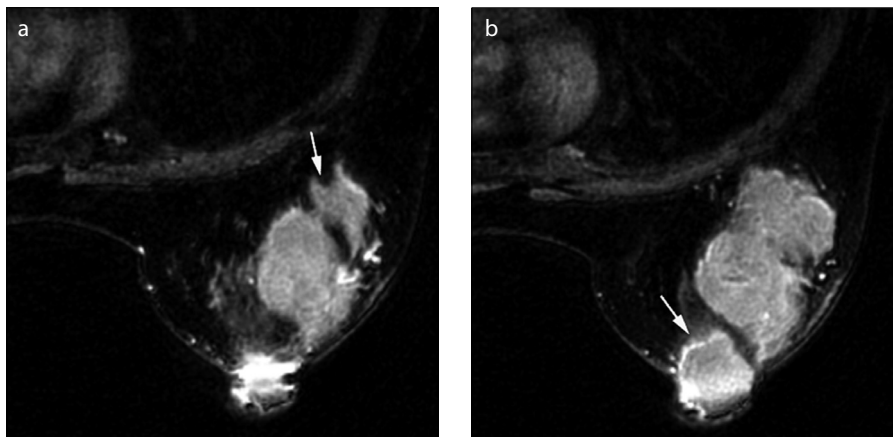


**Figure 1. a, b.** A 57-year-old woman (Case 6) with a palpable mass in the right breast for one month and nipple enlargement for two weeks. Axial T1-weighted contrast-enhanced image reveals multiple masses with homogeneous enhancement and spiculated margins (arrow, a) as well as nipple enlargement (arrow, b) in the right breast. The lesions in the breast and the nipple shrank markedly after four times of chemotherapy (not shown).

in previous reports (1, 2, 4–23). Although the prevalence of nipple enlargement is low, this sign could alert the radiologist to consider the diagnosis of lymphoma.

MRI findings of previously reported patients with breast lymphoma (Table 3) varies (4, 7–22). Breast lymphomas commonly showed isointense signal on T1-weighted

imaging and slightly hyperintense signal on T2-weighted imaging (8, 22). Matsubayashi et al. (21) found hypointense or hyperintense signal with linear or band-like structures on STIR images, corresponding to fibrous bands with vessels and/or edematous changes in breast lymphomas. In our case series, two masses subjected to STIR showed hypointense or isointense signal, but no septa were found, possibly due to the limited number of cases. Surov et al. (8) reported that breast lymphomas were likely to be round or oval masses with well-defined margins on MRI. However, Liu et al. (22) revealed that breast lymphomas more commonly had an irregular margin. In our study, all of the masses had irregular or spiculated margins. The difference in findings may be due to the higher spatial resolution of MRI systems used in our study. We reviewed all pathologic findings and found no marked desmoplasia or scirrhous reactions, in accordance with the

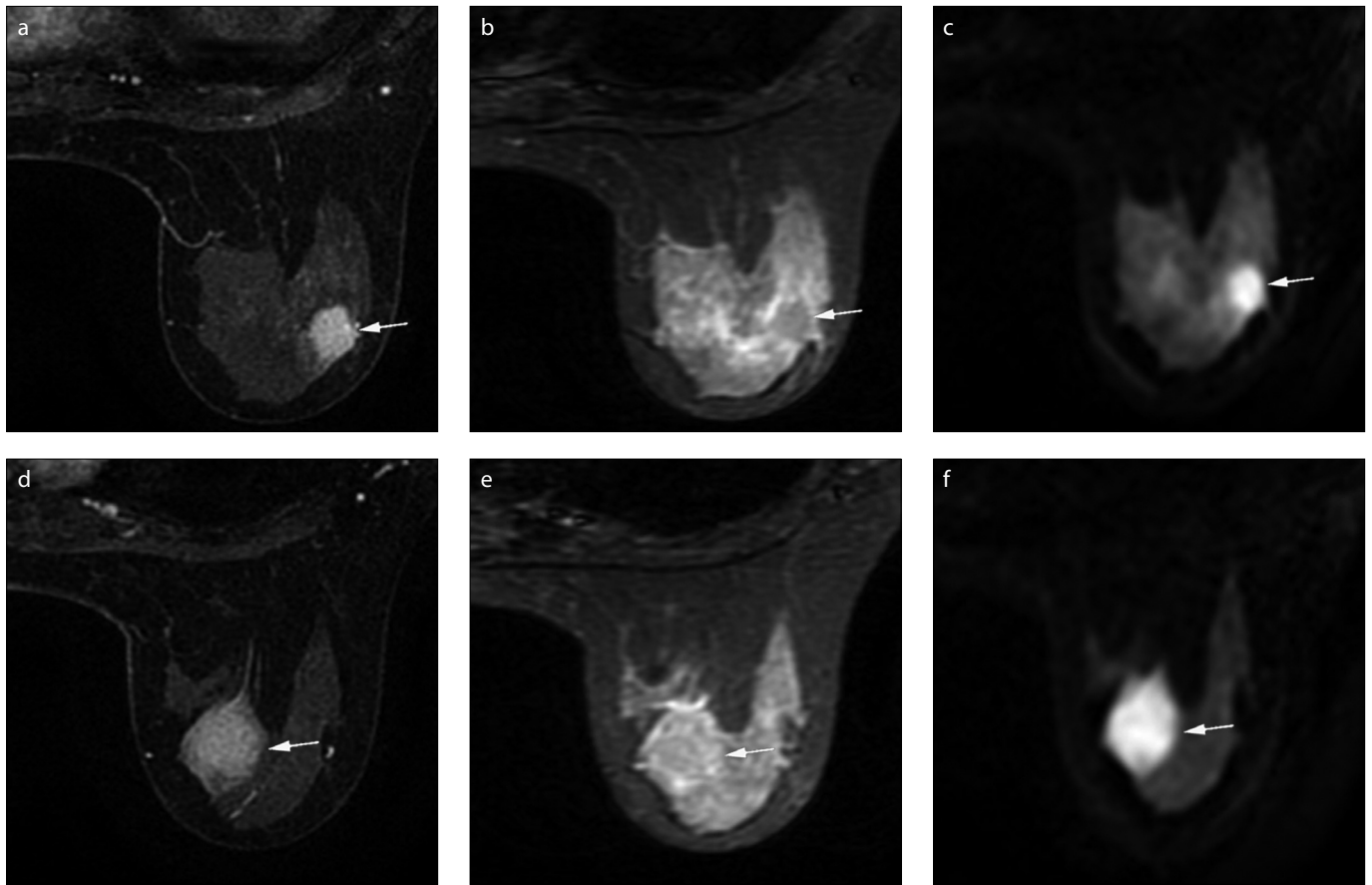


**Figure 2. a–f.** A 70-year-old woman (Case 7) with a palpable mass in the right breast for two days. Axial T1-weighted contrast-enhanced image (a) reveals an oval mass (arrow) with irregular margins in the upper outer quadrant of the right breast. The mass presents hypointense signal (arrow) compared with the surrounding fibroglandular tissue on short tau inversion recovery (STIR) image (b). Diffusion-weighted imaging (DWI) (c) demonstrates a hyperintense mass with a mean apparent diffusion coefficient (ADC) value of  $0.867 \times 10^{-3} \text{ mm}^2/\text{s}$ . Axial T1-weighted contrast-enhanced MRI (d) reveals an additional round mass (arrow) with irregular margins in the upper inner quadrant of the right breast. This mass was not detected on ultrasonography. The mass presents with isointense signal (arrow) compared with the surrounding fibroglandular tissue on STIR image (e). The mass presents with hyperintense signal (arrow) on DWI (f) and has a mean ADC value of  $0.732 \times 10^{-3} \text{ mm}^2/\text{s}$ .

previous study (30). Although grossly circumscribed, breast lymphomas usually had an infiltrating border (3). For this reason, we postulate that the infiltrative growth pattern is responsible for the irregular or spiculated margin. The internal enhancement of breast lymphoma was more commonly homogeneous or mildly heterogeneous, while rim enhancement was rarely seen (4, 7–22), which is similar to the enhancement pattern of lymphomas in other sites. In the present study, most of the lesions had a homogeneous enhancement, which is consistent with the findings of previous studies.

Many studies reported a rapid initial enhancement and a plateau kinetic curve pattern for breast lymphomas (8, 20, 22). However, most of our cases had a medium initial enhancement and a washout pattern. Adjacent vessel sign commonly occurred in this study. As we know, the plateau or washout kinetic curve pattern and adjacent ves-

sel sign can also be seen in other malignant breast tumors and rarely in some benign conditions (28, 29). Therefore, none of these is pathognomonic for breast lymphoma. Matsubayashi et al. (21) suggested that the penetrating vessel was a useful diagnostic clue for breast lymphoma. In our series, the prevalence of this sign was low (25%); moreover, reports about the prevalence of this sign in other breast lesions are limited. Therefore, a prospective MRI study is needed to evaluate the prevalence of penetrating vessel sign in benign and malignant breast conditions.

Breast lymphoma often shows malignant features such as irregular or spiculated margins and a washout pattern in the delayed phase, making it difficult to differentiate from the other malignant breast tumors. In this condition, DWI may be a problem-solving tool. Although there were some overlaps, the ADC values of lymphoma were lower than those of glioblastoma

in the brain (24). The mean ADC value was statistically significantly lower in lymphoma than in undifferentiated nasopharyngeal carcinoma and squamous cell carcinoma (25). Lymphoma is a hypercellular tumor; therefore, it has a lower ADC value compared with other malignant tumors (24, 25). The mean ADC value of diffuse large B-cell lymphoma was reported as  $0.70 \times 10^{-3} \text{ mm}^2/\text{s}$  in other sites such as abdomen, neck, thorax, and thigh (31). In our study, the ADC values of breast lymphoma in one case with two masses were  $0.867 \times 10^{-3} \text{ mm}^2/\text{s}$  and  $0.732 \times 10^{-3} \text{ mm}^2/\text{s}$ , respectively, which were consistent with those of lymphoma in other sites (24, 25, 31). Partridge et al. (32) reported that at a b value of  $600 \text{ s}/\text{mm}^2$ , the ADC values of benign and malignant breast lesions were  $1.70 \pm 0.44 \times 10^{-3} \text{ mm}^2/\text{s}$  and  $1.31 \pm 0.27 \times 10^{-3} \text{ mm}^2/\text{s}$ , respectively. The malignant breast lesions in Partridge et al. (32) included ductal carcinoma in situ

(DCIS), invasive ductal carcinoma (IDC), and invasive lobular carcinoma (ILC). In contrast to the aforementioned study, the ADC values of breast lymphomas in our study were markedly lower than those of benign lesions and other malignant breast lesions such as DCIS, IDC, and ILC. The differences in ADC values between lymphoma and benign and other malignant conditions may help the differential diagnosis. However, the influence of different imaging systems and sequence parameters on the ADC value should be considered. Therefore future studies performed on single MRI platform with larger series of breast lymphomas and a variety of breast lesions are required for a more reliable conclusion.

On mammography, three imaging patterns could be detected as follows: mass, focal or global architectural distortion, and mammography without abnormalities (33). Most breast lymphomas could be detected by mammography and only 4%–13% of breast lymphoma showed no abnormalities on mammography (6–8). In our study, all patients who had undergone preoperative mammography had a positive finding. Breast lymphomas presented more commonly as hypoechoic masses with noncircumscribed margin on ultrasonography, which is in agreement with the previous series (6–8). MRI was reported to detect more lesions than ultrasonography (4, 9, 12, 14, 17). In the present study, in cases 1, 5, and 7, MRI detected more lesions than ultrasonography, similar to previous reports. MRI may be more sensitive in detecting multifocal or multicentric lesions of a breast lymphoma. Thus, when a breast lymphoma is suspected or confirmed, MRI could be recommended for a more accurate comprehensive assessment.

The principal limitation of our study is its small sample size. Another limitation is the use of two different MRI scanners with different sequences and presence of only one patient who underwent DWI. A multicenter study with a larger sample size and a single MRI system is needed to verify the value of DWI for differentiating breast lymphoma from other breast lesions.

In conclusion, the breast lymphomas in this group commonly showed a homogeneously enhancing mass with irregular margins and a washout curve pattern. A low ADC value obtained from DWI may indicate a possible diagnosis of breast lymphoma.

Furthermore, MRI may be more sensitive in detecting multifocal or multicentric lesions of breast lymphoma.

### Acknowledgements

The authors thank Bosong Wang for his assistance on statistics. This study was funded by the National Natural Science Foundation of China (NSFC 81371621). The funders had no role in study design, data collection and analysis, decision to publish, or preparation of the manuscript.

### Conflict of interest disclosure

The authors declared no conflicts of interest.

### References

1. Jeanneret-Sozzi W, Taghian A, Epelbaum R, et al. Primary breast lymphoma: patient profile, outcome and prognostic factors. A multicentre Rare Cancer Network study. *BMC Cancer* 2008; 8:86. [CrossRef]
2. Wiseman C, Liao KT. Primary lymphoma of the breast. *Cancer* 1972; 29:1705–1712. [CrossRef]
3. Lakhani SR, Ellis IO, Schnitt SJ, Tan PH, Van de Vijver MJ. WHO classification of tumours of the breast. *Lyon:IARC*, 2012; 156–160.
4. Oya M, Hirahashi M, Ochi M, et al. Spontaneous regression of primary breast lymphoma. *Pathol Int* 2009; 59:664–669. [CrossRef]
5. Jennings WC, Baker RS, Murray SS, et al. Primary breast lymphoma: the role of mastectomy and the importance of lymph node status. *Ann Surg* 2007; 245:784–789. [CrossRef]
6. Liberman L, Giess CS, Dershaw DD, Louie DC, Deutch BM. Non-Hodgkin lymphoma of the breast: imaging characteristics and correlation with histopathologic findings. *Radiology* 1994; 192:157–160. [CrossRef]
7. Yang WT, Lane DL, Le-Petross HT, Abruzzo LV, Macapinlac HA. Breast lymphoma: imaging findings of 32 tumors in 27 patients. *Radiology* 2007; 245:692–702. [CrossRef]
8. Surov A, Holzhausen HJ, Wienke A, et al. Primary and secondary breast lymphoma: prevalence, clinical signs and radiological features. *Br J Radiol* 2012; 85:e195–205. [CrossRef]
9. Mussurakis S, Carleton PJ, Turnbull LW. MR imaging of primary non-Hodgkin's breast lymphoma. A case report. *Acta Radiol* 1997; 38:104–107. [CrossRef]
10. Darnell A, Gallardo X, Sentis M, Castañer E, Fernandez E, Villajos M. Primary lymphoma of the breast: MR imaging features. A case report. *Magn Reson Imaging* 1999; 17:479–482. [CrossRef]
11. Demirkazik FB. MR imaging features of breast lymphoma. *Eur J Radiol* 2002; 42:62–64. [CrossRef]
12. Espinosa LA, Daniel BL, Jeffrey SS, Nowels KW, Ikeda DM. MRI features of mucosa-associated lymphoid tissue lymphoma in the breast. *AJR Am J Roentgenol* 2005; 185:199–202. [CrossRef]
13. Woo OH, Yong HS, Shin BK, Park CM, Kang EY. Synchronous bilateral primary breast lymphoma: MRI and pathologic findings. *Breast J* 2007; 13:429–430. [CrossRef]
14. Zechmann CM, Buchheidt D, Hildenbrand R, Teubner J. B-cell lymphoma of the female breast: comparison of mammography, ultrasound and dynamic MRI. *Ultraschall Med* 2010; 31:71–73. [CrossRef]

15. Adrada BE, Carkaci S, Whitman GJ. Case of the season: Large B-cell lymphoma involving both breasts. *Semin Roentgenol* 2011; 46:242–244. [CrossRef]
16. Rathod J, Taori K, Disawal A, et al. A rare case of male primary breast lymphoma. *J Breast Cancer* 2011; 14:333–336. [CrossRef]
17. Jinming X, Qi Z, Xiaoming Z, Jianming T. Primary non-Hodgkin's lymphoma of the breast: mammography, ultrasound, MRI and pathologic findings. *Future Oncol* 2012; 8:105–109. [CrossRef]
18. Uematsu T, Kasami M. 3T-MRI, elastography, digital mammography, and FDG-PET CT findings of subcutaneous panniculitis-like T-cell lymphoma (SPTCL) of the breast. *Jpn J Radiol* 2012; 30:766–771. [CrossRef]
19. Nakatsuka S, Uchiyama C, Okishiro M, et al. Primary diffuse large B-cell lymphoma of the nipple: a rare case of breast lymphoma localized in the nipple. *Breast J* 2013; 19: 199–200. [CrossRef]
20. Rizzo S, Preda L, Villa G, et al. Magnetic resonance imaging of primary breast lymphoma. *Radiol Med* 2009; 114:915–924. [CrossRef]
21. Matsubayashi RN, Inoue Y, Okamura S, Momosaki S, Nakazono T, Muranaka T. MR imaging of malignant primary breast lymphoma: including diffusion-weighted, histological features, and a literature review. *Jpn J Radiol* 2013; 31:668–676. [CrossRef]
22. Liu K, Xie P, Peng W, Zhou Z. The features of breast lymphoma on MRI. *Br J Radiol* 2013; 86:20130220. [CrossRef]
23. Shim E, Song SE, Seo BK, Kim YS, Son GS. Lymphoma affecting the breast: a pictorial review of multimodal imaging findings. *J Breast Cancer* 2013; 16:254–265. [CrossRef]
24. Doskaliyev A, Yamasaki F, Ohtaki M, et al. Lymphomas and glioblastomas: differences in the apparent diffusion coefficient evaluated with high b-value diffusion-weighted magnetic resonance imaging at 3T. *Eur J Radiol* 2012; 81:339–344. [CrossRef]
25. Fong D, Bhatia KS, Yeung D, King AD. Diagnostic accuracy of diffusion-weighted MR imaging for nasopharyngeal carcinoma, head and neck lymphoma and squamous cell carcinoma at the primary site. *Oral Oncol* 2010; 46:603–606. [CrossRef]
26. Wang L, Wang D, Fei X, et al. A rim-enhanced mass with central cystic changes on MR imaging: how to distinguish breast cancer from inflammatory breast diseases? *PLoS One* 2014; 9:e90355. [CrossRef]
27. D'Orsi CJ, Sickles EA, Mendelson EB, et al. ACR BI-RADS® Atlas, Breast Imaging Reporting and Data System. Reston, VA, American College of Radiology; 2013.
28. Dietzel M, Baltzer PA, Vag T, et al. The adjacent vessel sign on breast MRI: new data and a subgroup analysis for 1,084 histologically verified cases. *Korean J Radiol* 2010; 11:178–186. [CrossRef]
29. Han M, Kim TH, Kang DK, Kim KS, Yim H. Prognostic role of MRI enhancement features in patients with breast cancer: value of adjacent vessel sign and increased ipsilateral whole-breast vascularity. *AJR Am J Roentgenol* 2012; 199:921–928. [CrossRef]

30. Sabaté JM, Gomez A, Torruba S, et al. Lymphoma of the breast: clinical and radiological features with pathologic correlation in 28 patients. *Breast J* 2002; 8:294–304. [\[CrossRef\]](#)
31. Wu X, Pertovaara H, Dastidar P, et al. ADC measurements in diffuse large B-cell lymphoma and follicular lymphoma. *Eur J Radiol* 2013; 82:e158–164.
32. Partridge SC, DeMartini WB, Kurland BF, Eby PR, White SW, Lehman CD. Quantitative diffusion-weighted imaging as an adjunct to conventional breast MRI for improved positive predictive value. *AJR Am J Roentgenol* 2009; 193:1716–1722. [\[CrossRef\]](#)
33. Surov A. Imaging findings of hematologic diseases affecting the breast. *Semin Ultrasound CT MR* 2013; 34:550–557. [\[CrossRef\]](#)